MAXIMAL OIL RECOVERY FROM VIRGIN RESERVOIRS UNDER THREE-PHASE FLOW CONDITIONS

A. V. AZEVEDO, A. J. DE SOUZA, F. FURTADO, D. MARCHESIN, AND B. PLOHR

Abstract. If two fluids are available to displace oil from a virgin reservoir, what is the injection strategy that maximizes recovery? This question is considered here. Suppose that the densities of the oil in the reservoir and the two injected fluids are similar, so that gravity segregation can be neglected; and suppose that the injected fluids and the oil form three immiscible phases with no mass interchanges. What is the mixing proportion for injected fluid slugs that optimizes the oil recovery?

We derive formulae for the optimal injection proportion and oil recovery for Corey-type quadratic permeabilities. The optimal quantities are essentially determined by the viscosities of the three phases. The formulae are based on a recently-developed method-of-characteristics theory for immiscible three-phase flow. We present numerical simulations to illustrate this theory and the dependence of the saturation profiles and production histories on the injection proportion. We also show simulations that demonstrate how alternating injection of pure fluids in this proportion yields the same oil recovery.

1. Introduction

As is well known, the efficiency of oil recovery can be increased by injecting a mixture of two fluid phases instead of a single pure phase. Determining the mixing proportion that optimizes oil recovery requires finding solutions for the three-phase flow generalization of Buckley-Leverett's two-phase injection problem. The main result of this paper is a formula for this optimal proportion.

We consider the injection of a mixture of two fluids into a thin cylinder of porous rock that is initially saturated with pure oil. For concreteness, we call the injected fluids water and gas, although they could be any two fluids that are immiscible with oil and each other. For simplicity, we assume that the three phases are incompressible, that gravitational segregation and capillarity effects are negligible, and that there is no mass transfer among the phases. The mobility of each phase is assumed to be proportional to the square of its own saturation and inversely proportional to the phase viscosity. (This particular Corey permeability model is conducive to analysis and generalizes the well known examples of Buckley and Leverett [4, 6].) The mathematical model consists of two conservation laws representing Darcy's law combined with mass conservation for two of the phases. As we do not make any prior assumption about the phase viscosities, the flow problem depends on two dimensionless parameters, such as two of the viscosity ratios.

Key words and phrases. method of characteristics, Buckley-Leverett solution, immiscible three-phase flow, three-phase permeabilities.

This work was supported in part by: FEMAT under Grant 04/10, UnB under Grant FUNPE 2005, CNPq under Grants 620029/2004-8, 306609/2004-5, 620017/2004-0, 491148/2005-4, 304168/2006-8, 620025/2006-9, 472067/2006-0; Instituto do Milênio IM/AGIMB; FAPERJ under Grant E-26/152.525/2006; and the U. S. Department of Energy. The authors gratefully acknowledge the hospitality of IMPA, UFCG, UnB and UWyo during this work .

We find analytical solutions for such flow problems. There are two generic types of flows, which are separated by a critical flow. In the critical flow, for which the injection proportion is the water/gas viscosity ratio, the water/gas proportion remains constant in space and time. In one of the generic flows, the water/gas proportion is higher than the critical proportion; we say that such a flow is *water-dominated*. The other generic flow is *gas-dominated*, meaning that the water/gas proportion is lower than critical.

In all injection flows, there is a faster shock wave across which the oil saturation decreases discontinuously. Generically, a two-phase water/oil or gas/oil mixture is left behind, depending on whether the flow is water- or gas-dominated. Trailing the fast shock wave, there is, in general, a slower shock wave and a smooth profile reaching back to the injection state, which is similar to the Buckley-Leverett profile for two-phase flow. Breakthrough of the injected fluid occurs when the faster shock wave arrives at the production point.

If fluid is injected at the critical proportion, the two shock waves coalesce and the whole profile resembles the Buckley-Leverett profile. The maximal recovery up to breakthrough is attained when fluid is injected precisely at the critical proportion. When the two injected fluids have comparable viscosities, the gain in recovery over injection of a pure fluid is substantial.

In practice, it is difficult to inject two immiscible fluids simultaneously at a specified mixture proportion. Instead, one can inject them alternately in the appropriate proportions. (This injection strategy is called WAG, for water-alternating-gas.) Because of fluid mixing within the porous rock, the critical proportion is attained sufficiently far downstream of the injection point (see, *e.g.*, Ref. [9]). We present numerical simulations of this recovery strategy that demonstrate how maximal recovery can indeed be attained using WAG.

The overall picture is essentially unchanged in a class of models more general than the Corey quadratic permeability model. This qualitative stability is justified in a companion paper, where numerical simulations, rather than explicit formulae, determine the solution profiles.

A Corey-type model loses strict hyperbolicity at an umbilic point. Models without umbilic points have been considered for three-phase flow; see Ref. [8]. They yield simple solutions for the injection problem. However, they are unrealistic because immiscibility of the three phases necessitates loss of strict hyperbolicity [13, 2, 10], *i.e.*, either umbilic points or elliptic regions are present. Models with umbilic points have complicated solutions, but are still well behaved mathematically; see Ref. [9] for a review of their properties. In this paper, we confront the extra complication entailed by the important physical property of immiscibility.

This paper is organized as follows. In Sec. 2, we describe our model, establish notation and recall relevant definitions. In Sec. 3, we show that, whatever the injected mixture is, the displacing fluid is separated from the *in situ* oil by a saturation discontinuity, which we call the lead shock wave. Two types of lead shock waves occur in generic flows: one in which the trailing fluid is a two-phase water/oil mixture, and the other in which it is a two-phase gas/oil mixture. Besides these two types of lead shock waves, there is a critical shock type, for which the displacing fluid is a critical mixture of oil, water and gas.

In Sec. 4, we study flows involving a critical shock wave. The solution profile consists of a rarefaction wave trailing the lead shock wave, just as in a two-phase Buckley-Leverett profile. Perturbing from a critical flow shows that a critical shock wave results from the coalescence of a slow-family shock wave with a fast-family shock wave. As such, a critical shock wave displaces more oil than either of these two shock waves individually; in fact, it optimizes

recovery up to the breakthrough time. We provide explicit formulae for the critical injection proportion, oil recovery, and breakthrough time.

In Sec. 5, we present evidence that the general solutions in our model have the same type (water- or gas-dominated) as the injection mixture. (We describe in detail only water-dominated flows, as gas-dominated flows are analogous.) The main feature of these flows is the occurrence of both a fast-family shock wave and a slow-family shock wave. In Sec. 6, we show results from numerical simulations of WAG recovery that demonstrate how this strategy can achieve maximal oil recovery.

In Sec. 7, we discuss a three-phase flow model that does not exhibit the bifurcation into water- and gas-dominated types. We argue that the bifurcation is absent from this model because it is strictly hyperbolic, which in turn is caused by a permeability model such that one phase becomes miscible at low saturation. We also summarize our results and explain how they generalize when the permeabilities do not have the simple quadratic form.

2. Mathematical Model

Consider the flow of a mixture of three fluid phases (which, for concreteness, are called water, oil and gas) in a thin, horizontal cylinder of porous rock. Let $s_{\mathrm{w}}(x,t)$, $s_{\mathrm{g}}(x,t)$ and $s_{\mathrm{o}}(x,t)$ denote the respective saturations at distance x along the cylinder, at time t. Because $s_{\mathrm{w}}+s_{\mathrm{g}}+s_{\mathrm{o}}=1$ and $0\le s_{\mathrm{w}}, s_{\mathrm{o}}, s_{\mathrm{g}}\le 1$, we depict the space of states of the fluid mixture as the saturation triangle; see Fig. 1. In our analysis, we choose s_{w} and s_{g} as the two independent coordinates.

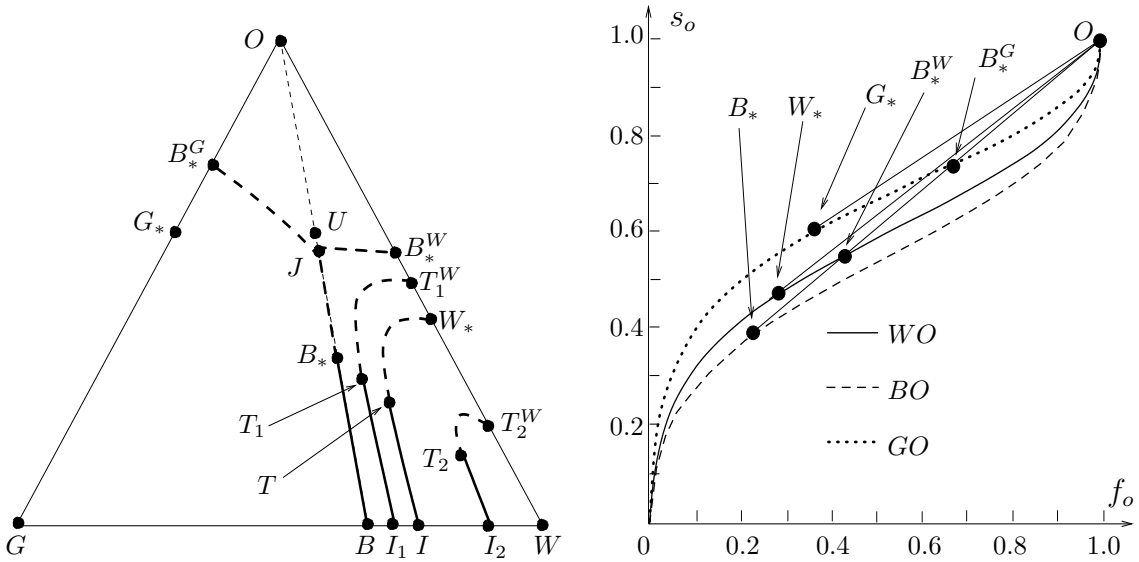

FIGURE 1. Left: saturation triangle. Solution paths from injection states B, I_1, I, and I_2 to O. The solid curves to B_*, T_1, T, and T_2 represent slow-family rarefaction waves. The pairs (T_1, T_1^W), (T, W_*), and (T_2, T_2^W) define slow-family shock waves. The path (T_2^W, W_*) represents a fast-family rarefaction wave; the pairs from W_* and T_1^W to O define fast-family shock waves. The shock wave (B_*, O) belongs to the critical profile. The role of B_*^W and B_*^G is explained in Sec. 4. Right: Welge's construction of the states G_*, W_*, and B_* for the oil fractional flow function on the invariant edges and line.

We intend to understand flows relevant to enhanced oil recovery, as applied to a reservoir that has never undergone production. Therefore we assume that the porous rock cylinder initially contains pure oil, and imagine injecting a specific mixture of the so-called water and gas into the left end of the cylinder. Later, in Sec. 6, we consider alternating injection of water and gas (WAG).

2.1. **Conservation laws.** Three-phase flow is governed by the non-dimensionalized system

$$\frac{\partial s_{\mathrm{w}}}{\partial t} + \frac{\partial f_{\mathrm{w}}(s_{\mathrm{w}}, s_{\mathrm{g}})}{\partial x} = 0, \tag{2.1}$$

$$\frac{\partial s_{\mathrm{g}}}{\partial t} + \frac{\partial f_{\mathrm{g}}(s_{\mathrm{w}}, s_{\mathrm{g}})}{\partial x} = 0 \tag{2.2}$$

representing conservation of water and gas. The fractional flow functions $f_{\mathrm{w}}(s_{\mathrm{w}}, s_{\mathrm{g}})$ and $f_{\mathrm{g}}(s_{\mathrm{w}}, s_{\mathrm{g}})$ are determined by the relative permeabilities of the three phases.

Although each fluid phase becomes immobile below an irreducible saturation, a model of three-phase flow can be remapped so that the irreducible saturations are zero; see, *e.g.*, Ref. [8]. Therefore we assume that the relative permeabilities are strictly positive within the saturation triangle. (In other words, s_{w}, s_{g}, and s_{o} are reduced saturations.)

In this paper, we specialize to the Corey model for the permeabilities. With this choice, we can highlight the phenomena of interest while avoiding complicated analysis. (We expect that solutions for more realistic models are qualitatively similar to those of Corey models.) Explicitly, the fractional flow functions we adopt are

$$f_{\mathrm{w}}(s_{\mathrm{w}}, s_{\mathrm{g}}) := \frac{s_{\mathrm{w}}^2/\mu_{\mathrm{w}}}{\lambda(s_{\mathrm{w}}, s_{\mathrm{g}})} \qquad \text{and} \qquad f_{\mathrm{g}}(s_{\mathrm{w}}, s_{\mathrm{g}}) := \frac{s_{\mathrm{g}}^2/\mu_{\mathrm{g}}}{\lambda(s_{\mathrm{w}}, s_{\mathrm{g}})}. \tag{2.3}$$

Here the constants μ_{w}, μ_{g}, and μ_{o} are the water, gas, and oil phase viscosities, respectively, and

$$\lambda(s_{\mathrm{w}}, s_{\mathrm{g}}) := s_{\mathrm{w}}^2/\mu_{\mathrm{w}} + s_{\mathrm{g}}^2/\mu_{\mathrm{g}} + s_{\mathrm{o}}^2/\mu_{\mathrm{o}}, \qquad \text{where} \quad s_{\mathrm{o}} = 1 - s_{\mathrm{w}} - s_{\mathrm{g}}, \tag{2.4}$$

is the total mobility.

2.2. **Basic solutions.** Equations (2.1)–(2.2) have solutions that propagate as waves. The propagation speeds of continuous waves are the two eigenvalues of the Jacobian derivative matrix

$$J(s_{\mathrm{w}}, s_{\mathrm{g}}) := \frac{\partial\,(f_{\mathrm{w}}, f_{\mathrm{g}})}{\partial\,(s_{\mathrm{w}}, s_{\mathrm{g}})}, \tag{2.5}$$

provided that these eigenvalues are real, in which case the smaller is called the slow characteristic speed $\lambda_{\mathrm{s}}(s_{\mathrm{w}}, s_{\mathrm{g}})$ and the larger is called the fast-family characteristic speed $\lambda_{\mathrm{f}}(s_{\mathrm{w}}, s_{\mathrm{g}})$. For the Corey model, both eigenvalues are real and nonnegative for each state in the saturation triangle.

The Corey model does, however, have the peculiarity that, for a unique state in the interior of the saturation triangle (labeled U in Fig. 1), the two characteristic speeds coincide. Such a state is called an umbilic point. The state U is determined by the viscosity of the fluid phases: $s_{\mathrm{w}}(U) = \mu_{\mathrm{w}}/\mu_{\mathrm{tot}}$, $s_{\mathrm{g}}(U) = \mu_{\mathrm{g}}/\mu_{\mathrm{tot}}$, and $s_{\mathrm{o}}(U) = \mu_{\mathrm{o}}/\mu_{\mathrm{tot}}$, where $\mu_{\mathrm{tot}} = \mu_{\mathrm{w}} + \mu_{\mathrm{g}} + \mu_{\mathrm{o}}$. We shall see that the line through O and U plays a central role in the construction of solutions.

System (2.1)–(2.2) has continuous solutions called slow-family rarefaction waves. For such a solution, $\lambda_{\mathrm{s}}(s_{\mathrm{w}}, s_{\mathrm{g}}) = x/t$ and, as x varies for while $t > 0$ remains fixed, $(s_{\mathrm{w}}, s_{\mathrm{g}})$ follows a rarefaction curve in the saturation triangle. Similarly there are fast-family rarefaction waves.

This system also admits solutions that have jump discontinuities. For such a discontinuity, the state a just ahead of it (*i.e.*, downstream), the state b just behind it, and its propagation speed σ are constrained by the Rankine-Hugoniot (RH) condition

$$-\sigma\left(s_{\mathrm{w}}^{a}-s_{\mathrm{w}}^{b}\right)+f_{\mathrm{w}}(s_{\mathrm{w}}^{a},s_{\mathrm{g}}^{a})-f_{\mathrm{w}}(s_{\mathrm{w}}^{b},s_{\mathrm{g}}^{b})=0, \tag{2.6}$$

$$-\sigma\left(s_{\mathrm{g}}^{a}-s_{\mathrm{g}}^{b}\right)+f_{\mathrm{g}}(s_{\mathrm{w}}^{a},s_{\mathrm{g}}^{a})-f_{\mathrm{g}}(s_{\mathrm{w}}^{b},s_{\mathrm{g}}^{b})=0. \tag{2.7}$$

If, in addition, a jump discontinuity obeys a physical admissibility criterion, then it is called a shock wave. Admissibility for two-phase flow (*i.e.*, for a scalar conservation law) is discussed in Sec. 2.4. Admissibility for systems of conservation laws such as system (2.1)–(2.2) is discussed in Ref. [1].

Notice that if the RH condition between states a and b holds with a certain speed σ, and it also holds for the same speed between states b and c, it is easy to see that the RH condition is satisfied between states a and c with the same speed. This is the essence of the triple-shock rule [7].

2.3. **Two-phase flow.** In the simplest experiment, pure water (state W, with $s_{\mathrm{w}}(W)=1$) is injected into the cylinder, which is saturated with oil (state O, with $s_{\mathrm{o}}(O)=1$). The result is two-phase flow involving only states that lie along the water/oil edge W-O of the saturation triangle in Fig. 1. For the purpose of establishing useful notation, we review this kind of flow.

If $s_{\mathrm{g}}=0$ initially, then because $f_{\mathrm{g}}(s_{\mathrm{w}},0)=0$, Eq. (2.2) implies that s_{g} remains zero. In other words, the water/oil edge of the saturation triangle is invariant. By substituting $s_{\mathrm{g}}=0$ into Eq. (2.1), the first of Eqs. (2.3), and Eq. (2.4) one obtains the equation for s_{w} on this edge. For generality of notation, let us omit the subscript "w"; then s represents the saturation of the injected fluid, which has phase viscosity μ, and $s_{\mathrm{o}}=1-s$. Thus we obtain the following single conservation law governing two-phase flow:

$$\frac{\partial s}{\partial t}+\frac{\partial f(s;\nu)}{\partial x}=0, \tag{2.8}$$

where

$$f(s;\nu):=\frac{s^{2}}{s^{2}+\nu(1-s)^{2}} \tag{2.9}$$

and the constant $\nu:=\mu/\mu_{\mathrm{o}}$ is the phase viscosity ratio. For states on the water/oil edge, the slow-family characteristic speed is zero, and the fast-family characteristic speed is $\mathrm{d}f(s;\nu)/\mathrm{d}s$. Moreover, one of the equations in the RH condition is satisfied trivially and the other reduces to

$$-\sigma\left(s^{a}-s^{b}\right)+f(s^{a};\nu)-f(s^{b};\nu)=0. \tag{2.10}$$

For example, the foregoing equations hold with $s:=s_{\mathrm{w}}$ and $\nu:=\mu_{\mathrm{w}}/\mu_{\mathrm{o}}$. Likewise, because the gas/oil edge G-O is invariant for a similar reason, these equations hold with $s:=s_{\mathrm{g}}$ and $\nu:=\mu_{\mathrm{g}}/\mu_{\mathrm{o}}$.

2.4. **Buckley-Leverett solution.** The flow that results when pure fluid ($s=1$, meaning either water or gas) is injected into the cylinder is the classical Buckley-Leverett solution. In this solution, a lead shock wave is followed by a continuous wave, with the shock speed matching the characteristic speed of the state just behind it.

The Welge tangency construction equates the characteristic speed with the shock speed: if s_* denotes the injected phase saturation just behind the shock wave, then at $s = s_*$:

$$\frac{\mathrm{d}f(s;\nu)}{\mathrm{d}s} = \frac{f(s;\nu)}{s}. \tag{2.11}$$

The solution of Eq. (2.11) and the corresponding shock speed are given respectively by

$$s = s_*(\nu) := \frac{1}{\sqrt{1+\nu^{-1}}} \qquad \text{and} \qquad \sigma = \sigma_*(\nu) := \frac{1+\sqrt{1+\nu^{-1}}}{2}. \tag{2.12}$$

This shock wave satisfies Oleĭnik's E-criterion [11], which requires, for a shock wave with $s^a < s^b$ to be admissible, that $[f(s;\nu) - f(s^a;\nu)]/(s - s^a) < \sigma$ for all s such that $s^a < s < s^b$. Among shock waves with $s^a = 0$ satisfying the E-condition, the one with $s^b = s_*(\nu)$ is the strongest and fastest. For this reason, we refer to it as the maximal shock wave.

The continuous wave trailing the shock wave in the Buckley-Leverett solution is a centered rarefaction wave. Within this wave, the fast-family characteristic speed equals x/t, so that the saturation $s(x,t)$ is given implicitly by the equation

$$\frac{\mathrm{d}f(s;\nu)}{\mathrm{d}s} = \frac{x}{t}. \tag{2.13}$$

If $t > 0$ is fixed, then s decreases continuously from $s = 1$ to $s = s_*(\nu)$ as x varies from the injection point to the position of the shock wave.

3. Lead Shock Wave

Return now to the three-phase flow in which a specific mixture of water and gas is injected into a porous rock cylinder initially containing pure oil. We first focus on the lead wave that displaces the *in situ* oil. In principle, this wave could be either a rarefaction wave or a shock wave. However, it cannot be a rarefaction wave ending at O: an easy calculation shows that characteristic speeds vanish at O in the saturation triangle, but are positive nearby.

3.1. **Hugoniot locus.**

The RH condition for a jump discontinuity with state O ahead reads

$$\sigma s_{\mathrm{w}} = \frac{s_{\mathrm{w}}^2/\mu_{\mathrm{w}}}{\lambda(s_{\mathrm{w}}, s_{\mathrm{g}})}, \qquad \sigma s_{\mathrm{g}} = \frac{s_g^2/\mu_{\mathrm{g}}}{\lambda(s_{\mathrm{w}}, s_{\mathrm{g}})}. \tag{3.1}$$

There are three types of solutions of these equations. For the first type, $s_{\mathrm{g}} = 0$, so that the second equation in (3.1) is satisfied trivially, whereas the first one determines σ in terms of $s_{\mathrm{w}} > 0$. Such a solution is a water/oil two-phase discontinuity. Similarly, the second type, for which $s_{\mathrm{w}} = 0$ and $s_{\mathrm{g}} > 0$, is a gas/oil two-phase discontinuity.

For the third type of solution, both s_{w} and s_{g} are nonzero. In (3.1), dividing the first equation by the second one yields

$$\frac{s_{\mathrm{w}}}{\mu_{\mathrm{w}}} = \frac{s_{\mathrm{g}}}{\mu_{\mathrm{g}}}. \tag{3.2}$$

The umbilic point U satisfies this equation, so that the solution set is the straight line segment B-O drawn in Fig. 1. Introducing the net water/gas saturation

$$s_{\mathrm{wg}} := s_{\mathrm{w}} + s_g = 1 - s_{\mathrm{o}}, \tag{3.3}$$

this line segment is conveniently parameterized as

$$s_{\mathrm{w}} = \frac{\mu_{\mathrm{w}}}{\mu_{\mathrm{wg}}} s_{\mathrm{wg}} \quad \text{and} \quad s_{\mathrm{g}} = \frac{\mu_{\mathrm{g}}}{\mu_{\mathrm{wg}}} s_{\mathrm{wg}}, \quad \text{where} \quad \mu_{\mathrm{wg}} := \mu_{\mathrm{w}} + \mu_{\mathrm{g}}, \tag{3.4}$$

for $0 \le s_{\rm wg} \le 1$. In other words, the Hugoniot locus of state O comprises the three line segments W-O, B-O, and G-O in Fig. 1.

3.2. **Invariance.** We have noted in Sec. 2.3 that the two-phase edges W-O and G-O of the saturation triangle are invariant. The line segment B-O is also invariant under the evolution governed by system (2.1)–(2.2). Indeed, substituting $s_{\rm w}$ and $s_{\rm g}$ from (3.4) into system (2.1)–(2.2), both equations reduce to the single Buckley-Leverett equation (2.8) with fractional flow function given by (2.9) with $s = s_{\rm wg}$ and $\nu = \mu_{\rm wg}/\mu_{\rm o}$. This reduction shows that if the solution path for the system (2.1)–(2.2) lies initially on the straight line B-O, its evolution continues on this line for all times. Therefore it is natural to refer to B-O as the invariant line segment. For more general immiscible three phase flows, such as Stone's model [3, 14], the invariant line segment is replaced by a curve that separates different types of solutions [1].

We refer to a solution lying entirely within W-B-O as a water-dominated solution, and similarly refer to gas-dominated solutions.

We have shown that the water/gas mixture in the proportions of Eq. (3.2) effectively behaves as a single phase; we can regard the flow of this phase and oil as another two-phase flow. We will take advantage of this fact in the discussion that follows.

3.3. **Maximal discontinuities.** We have demonstrated that the state behind the lead shock wave lies either on the invariant line segment or on one of the invariant edges. In each case, the discussion in Sec. 2.4 shows that this state must have oil saturation at least as large as that for the maximal shock wave given by Welge's construction (recall Sec. 2.4).

For the water/oil edge, the maximal shock wave is characterized by Eqs. (2.12) with $s := s_{\rm w}$ and $\nu := \mu_{\rm w}/\mu_{\rm o}$:

$$s_{\rm w}(W_*) = s_*(\mu_{\rm w}/\mu_{\rm o}), \quad s_{\rm o}(W_*) = 1 - s_{\rm w}(W_*), \quad \sigma(W_*, O) = \sigma_*(\mu_{\rm w}/\mu_{\rm o}). \tag{3.5}$$

Similar expressions hold for the gas/oil edge:

$$s_{\rm g}(G_*) = s_*(\mu_{\rm g}/\mu_{\rm o}), \quad s_{\rm o}(G_*) = 1 - s_{\rm g}(G_*), \quad \sigma(G_*, O) = \sigma_*(\mu_{\rm g}/\mu_{\rm o}). \tag{3.6}$$

For the invariant line segment, Eqs. (2.12) with $s := s_{\rm wg}$ and $\nu := \mu_{\rm wg}/\mu_{\rm o}$ imply that

$$s_{\rm wg}(B_*) = s_*(\mu_{\rm wg}/\mu_{\rm o}), \quad s_{\rm o}(B_*) = 1 - s_{\rm wg}(B_*), \quad \sigma(B_*, O) = \sigma_*(\mu_{\rm wg}/\mu_{\rm o}), \tag{3.7}$$

with the corresponding water and gas saturations obtained from Eqs. (3.4):

$$s_{\rm w}(B_*) = \frac{\mu_{\rm w}}{\mu_{\rm wg}}\, s_{\rm wg}(B_*) \qquad \text{and} \qquad s_{\rm g}(B_*) = \frac{\mu_{\rm g}}{\mu_{\rm wg}}\, s_{\rm wg}(B_*). \tag{3.8}$$

Equations (3.5), (3.6), and (3.8) define the coordinates of the states W_*, G_*, and B_* marked in Fig. 1 (left); Welge's construction for these states is illustrated in Fig. 1 (right). Notice that, in the latter figure, we draw $f_{\rm o} = 1 - f$ vs. $s_{\rm o} = 1 - s$ rather than f vs. s.

In summary, the amplitudes $s_{\rm wg}(B_*)$, $s_{\rm w}(W_*)$, $s_{\rm g}(G_*)$ of the maximal shock waves on the invariant line segment, the water/oil edge, and the gas/oil edge, respectively, are determined by the viscosity ratios $\mu_{\rm wg}/\mu_o$, $\mu_{\rm w}/\mu_o$, and $\mu_{\rm g}/\mu_o$. Assuming that $\mu_{\rm g} < \mu_{\rm w}$, these viscosity ratios are related by

$$\frac{\mu_{\rm g}}{\mu_o} < \frac{\mu_{\rm w}}{\mu_o} < \frac{\mu_{\rm wg}}{\mu_o}. \tag{3.9}$$

According to Eqs. (2.12), the shock amplitude $s_*(\nu)$ increases, and the shock speed $\sigma_*(\nu)$ decreases, as ν increases. Therefore the shock wave (B_*, O) is slowest and has largest amplitude, whereas (G_*, O) is fastest and has smallest amplitude. As illustrated in Fig. 1, B_* lies below W_*, which in turn lies below G_*.

Concerning the total oil recovery up to breakthrough of the lead wave, we conclude that maximal recovery occurs when the state behind the lead shock wave lies on the invariant line segment. We will see, in the next section, that maximal recovery occurs when the injected water/gas mixture has the proportion specified by Eq. (3.2). The same effect is achieved by alternating injection of water and gas in this proportion (see Sec. 6).

4. Critical Solution

When the injected mixture is state B in Fig. 1, the initial data lies within the invariant line segment. Therefore the flow is governed by the two-phase flow equation (2.8), with $s := s_{\mathrm{wg}}$ and $\nu := \mu_{\mathrm{wg}}/\mu_{\mathrm{o}}$. Hence there is a solution, which we call the Buckley-Leverett solution, consisting of the centered slow-family rarefaction wave from B to B_* trailing the shock wave from B_* to O.

Let us understand the shock wave (B_*, O) as a solution of the three-phase flow system (2.1)–(2.2). Its speed $\sigma(B_*, O)$ is given in Eq. (3.7). Any shock wave joining $(s_{\mathrm{w}}, s_{\mathrm{g}})$ to O with speed $\sigma(B_*, O)$ satisfies the RH condition (3.1) with $\sigma = \sigma(B_*, O)$. Besides the shock wave with left state B_* on the invariant line segment, there are two other shock waves with right state O and speed $\sigma(B_*, O)$, which have left states on the invariant edges, denoted by B_*^W and B_*^G. (Recall Sec. 3.1.) To find the left state on the edge $s_{\mathrm{g}} = 0$, we solve a version of the first of equations (3.1) with unknown s_{w}:

$$\sigma(B_*, O) = \frac{s_{\mathrm{w}}/\mu_{\mathrm{w}}}{\lambda(s_{\mathrm{w}}, 0)}. \tag{4.1}$$

This is a quadratic equation in s_{w}, which has precisely one root $s_{\mathrm{w}} = s_{\mathrm{w}}(B_*^W)$ less than $s_{\mathrm{w}}(W_*)$, giving rise to the state B_*^W. In a similar way, we find the state B_*^G on the edge $s_{\mathrm{w}} = 0$.

By the triple-shock rule mentioned in Sec. 2.2, each pair of states among O, B_*, B_*^W, and B_*^G defines a discontinuity with speed $\sigma(B_*, O)$. (Only some of these discontinuities represent admissible shock waves, however.) For instance, the shock wave (B_*, O) can be viewed alternatively as composed of two equal-speed shock waves (B_*, B_*^W) and (B_*^W, O). From this viewpoint, the solution, when mixture B is injected, comprises three waves: the slow-family rarefaction wave from B to B_* trailing the two shock waves (B_*, B_*^W) and (B_*^W, O). We call it the critical water-dominated solution. We shall see presently that the critical water-dominated solution remains "stable" when the fraction of water in the injected mixture is increased.

Similarly there is the critical gas-dominated solution comprising the slow-family rarefaction wave from B to B_* and the two shock waves (B_*, B_*^G) and (B_*^G, O). We emphasize, however, that fixed-time saturation profiles for the critical water- and gas-dominated solutions are indistinguishable from that for the Buckley-Leverett solution, which is shown in Fig. 3(b).

5. Water-Dominated Solutions

There are two extremal cases for water-dominated flows. When pure water is injected, the solution consists of the fast-family rarefaction wave from state W to state W_* and the shock

wave (W_*, O). This solution is the Buckley-Leverett solution reviewed in Sec. 2. The other extremal case is the critical water-dominated flow; the solution consists of the slow-family rarefaction wave from state B to state B_* trailing the two (coincident) shock waves (B_*, B_*^W) and (B_*^W, O). The two extremal solutions are illustrated in Fig. 1, in state space, and in Figs. 3(a) and 3(b), in physical space.

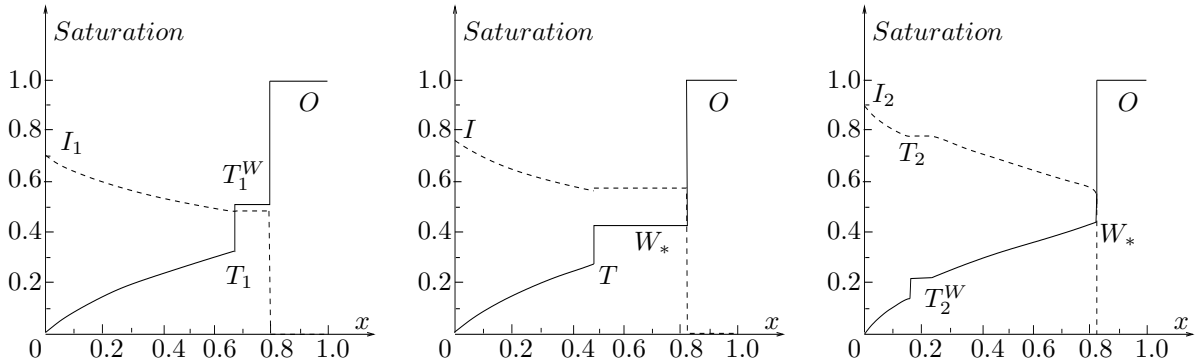

(a) I_1: $s_{\mathrm{w}} = 0.7$ (b) I: $s_{\mathrm{w}} = 0.764$ (c) I_2: $s_{\mathrm{w}} = 0.9$

FIGURE 2. Profiles for different injection states at the same PVI. Solid curves indicate oil saturations, whereas dashed curves indicate water saturations.

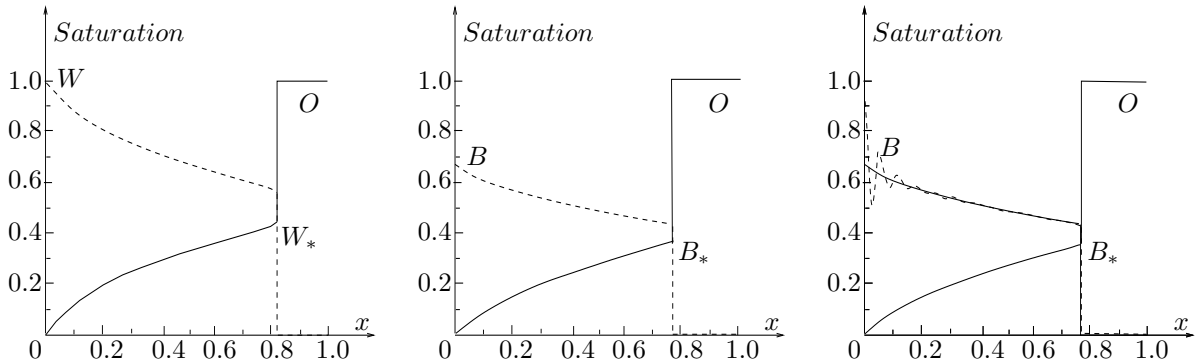

(a) W: $s_{\mathrm{w}} = 1$ (b) B: $s_{\mathrm{w}} = 2/3$ (c) Continuous & WAG injection.

FIGURE 3. Profiles for different injection regimes. Figures 3(a) and 3(b) are as in Fig. 2. See Sec. 6 for Fig. 3(c). States in Figs. 2 and 3 correspond to those in Fig. 1.

Imagine injecting a mixture I_1 having slightly higher fraction of water than B has. (Refer to Fig. 1 and Fig. 2(a).) In the corresponding solution, there is a slow-family rarefaction wave from I_1 to a state T_1 near B_* such that a shock wave with speed $\lambda_{\mathrm{s}}(T_1)$ leads from T_1 to some state T_1^W on the water/oil edge; here T_1^W lies slightly below B_*^W. The shock wave (T_1, T_1^W) trails the shock wave (T_1^W, O), which is strictly faster, so that a constant region with state T_1^W appears between them. As I_1 tends to B, the shock waves (T_1, T_1^W) and (T_1^W, O) approach, respectively, the equal-speed shock waves (B_*, B_*^W) and (B_*^W, O). A proof of these assertions is shown in Ref. [1].

The solution is qualitatively different if the injection mixture I_2 has high enough water fraction that the corresponding state T_2^W lies below W_*, as indicated in Fig. 1. Like for states I_1, there is a slow-family rarefaction wave from I_2 to a state T_2; a shock wave with speed $\lambda_s(T_2)$ from T_2 to a state T_2^W; and a constant region with state T_2^W. Now, however, a fast-family rarefaction wave leads from T_2^W to W_*, and then a shock wave joins W_* to O. See the solution profile in Fig. 2(c).

Separating solutions with injection states I_1 from those with injection states I_2 is the solution with injection state I, which contains the maximal shock wave (W_*, O), but not a fast-family rarefaction wave. See Fig. 2(b).

In the solutions just described, the lead wave is the shock wave from either T_1^W or W_* to O. Total oil recovery up to breakthrough of the lead wave is maximized by the critical injection conditions, when the lead shock wave (B_*^W, O) is slowest. As the fraction of water in the injected mixture is increased from its value for B, the speed of the lead shock wave increases, and hence oil recovery decreases. However, if the injected water fraction exceeds a certain level, corresponding to state I, then the lead shock wave is (W_*, O) and oil recovery is independent of the water fraction; in fact, the oil recovery is the same as when pure water is injected.

Critical recovery is significantly larger than pure-fluid recovery only when the viscosities of the injected fluids are comparable. This is the case for micellar flow [5]; however, Fig. 6 in that work indicates that the micro-emulsion relative permeability is not a quadratic. It could also be the case for foam injection [12]. Perhaps there exist circumstances in which one could take advantage of the slow-family shock for injection conditions given by I.

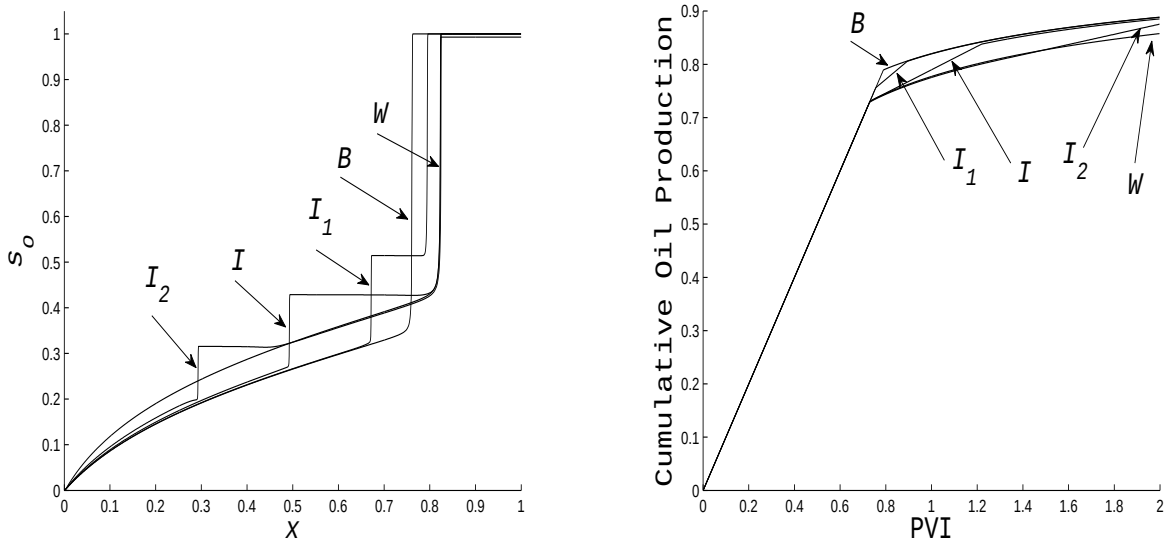

FIGURE 4. For different injection mixtures B, I_1, I, I_2, and W: oil-saturation profiles and production histories (on the right).

We summarize the results obtained so far in Fig. 4. We show oil profiles on the left and oil-production histories on the right. Initially, the oil production is dictated by the injection rate, which is the same for all the mixtures. At their respective breakthrough times, there is increasing recovery from the injection of pure water (state W), hypothetical mixtures

with increasing proportion of gas I_2, I, I_1 and the critical mixture B. Notice that recovery for injection mixtures with water saturations between I and B does not take too long to catch up with the critical recovery history, indicating that this is a good range for injection mixture proportions. Of course, there is an analogous range for gas-dominated flows where this catch-up phenomenon occurs. Outside of this good range around the critical injection proportion, the production history takes much longer to catch up with the critical recovery.

6. Simulations of WAG

When two fluids are injected alternately, the flow deep within the porous medium behaves as if an effective mixture were injected; see, *e.g.*, Ref. [9]. This phenomenon is confirmed in the WAG simulation shown in Fig. 3(c), where the time-averaged injection proportion equals the critical proportion. In this figure, there are two superimposed profiles corresponding to the same time. The first one is the result for continuous injection at the critical proportion; it is the same profile as in Fig. 3(b), except that the water saturation is shown as a solid curve in Fig. 3(c). The second profile is the result of the WAG simulation. The lower ramp shows the oil profiles for both continuous and WAG injection, which are indistinguishable. The upper oscillating dashed curve is the water saturation profile for WAG injection; far enough from the injection point, it becomes the same as that for continuous injection.

This simulation comparison illustrates that WAG with time-averaged injection proportion equal to the critical proportion yields essentially the same results as continuous injection at the critical proportion. Thus the WAG recovery strategy offers a way to achieve the maximal recovery described in the previous section. To be practical, however, a stringent limitation to the efficiency of WAG related to gravity segregation [12] must be overcome.

7. Discussion

A different model for three-phase flow was proposed in Ref. [8]. The main difference between this model and ours is that the gas permeability tends to zero linearly with the gas saturation, whereas in ours it tends to zero faster than linearly. We are of the opinion that the linear behavior does not correctly account for the genuine immiscibility of the gas in the other phases. This issue was studied mathematically in Ref. [2].

As a result of the linear behavior, the model in Ref. [8] is strictly hyperbolic in the interior of the saturation triangle. Referring to Fig. 1, it is as if the line segment B-O were pushed onto the edge W-O. In other words, the solutions of this model all look like the gas-dominated ones in our model, except when pure water is injected. In particular, the state behind the lead shock wave is always a gas/oil mixture. This feature suggests an experimental way of determining whether either of the two models is realistic. We also note that the difference between the flow profiles for the two models is biggest when the three phases have comparable viscosities.

In summary, we have determined the long-time behavior of saturation profiles when a mixture of two fluids is injected into porous rock that initially contains only oil. We have confirmed that such injection mixtures can be attained within the rock by alternating the injection of the two fluids. Neglecting gravity segregation, rock heterogeneity, hysteresis and fingering effects, and assuming the Corey quadratic permeability model, we have found an explicit formula for the injected fluid mixture proportion that leads to maximal oil recovery. We expect similar results for other genuinely immiscible three-phase flow models, such as Stone's model; the reason is that non-hyperbolic three-phase fluid mixtures do not appear in

the solutions we have constructed, so that these solutions ought to be stable under restricted changes to the permeabilities. This and other model generalizations will be the object of future study.

References

[1] A. Azevedo, A. de Souza, F. Furtado and D. Marchesin, *Mathematical aspects of a model for three-phase flow in porous media*, in preparation, (2008).

[2] A. Azevedo, D. Marchesin, B. Plohr and K. Zumbrun, *Capillary instability in models for three-phase flow*, Z. Angew. Math. Phys. **53** (2002), 713–746.

[3] K. Aziz and A. Settari, *Petroleum Reservoir Simulation*, Elsevier Applied Science, New York–London, 1990.

[4] S. Buckley and M. Leverett, *Mechanisms of fluid displacement in sands*, Trans. AIME, **146** (1942), 187–196.

[5] M. Delshad, G. Pope and L. Lake, *Two- and three-phase relative permeabilities of micellar fluids*, SPE J., **2** (1987), 327–337.

[6] R. Guzmán and F. J. Fayers, *Solutions to the three-phase flow Buckley-Leverett problem*, SPE 35156, **2** (1997), 301–311.

[7] E. Isaacson, D. Marchesin, B. Plohr and B. Temple, *Multiphase flow models with singular Riemann problems*, Comp. Appl. Math., **11** (1992), 147–166.

[8] R. Juanes and T. Patzek, *Relative permeabilities for strictly hyperbolic models of three-phase flow in porous media*, Transport in Porous Media, **57** (2004), 125–152.

[9] D. Marchesin and B. Plohr, *Wave structure in WAG recovery*, SPE J., **6** (2001), 209–219.

[10] H. Medeiros, *Stable hyperbolic singularities for three–phase flow models in oil reservoir simulation*, Acta Applicandae Mathematicae, **28**, (1992), 135–159.

[11] O. A. Oleĭnik, *Discontinuous solutions of non-linear differential equations*, Uspekhi Mat. Nauk, **12** (1957), 3–73; English translation in Amer. Math. Soc. Transl., ser. 2, **26** (1963), 95–172, 1957.

[12] W. R. Rossen and C. J. van Duijn, *Gravity segregation in steady-state horizontal flow in homogeneous reservoirs*, J. Pet. Sci. Eng., **43** (2004), 99–111.

[13] M. Shearer and J. Trangenstein, *Loss of real characteristics for models of three-phase flow in a porous medium*, Transport in Porous Media, **4** (1989), 499–525.

[14] H. Stone, *Probability model for estimating three-phase relative permeability*, J. Petr. Tech., **22** (1970), 214–218.

Departamento de Matemática, Universidade de Brasília, 70910-900 Brasília, DF, Brazil
E-mail address: arthur@mat.unb.br

Departamento de Matemática e Estatística, Universidade Federal de Campina Grande, 58109-970 , Campina Grande, PB, Brazil
E-mail address: cido@dme.ufcg.edu.br

Department of Mathematics, University of Wyoming, 82071-3036 Laramie, WY, USA
E-mail address: furtado@uwyo.edu

SPE and Instituto de Matemática Pura e Aplicada, Estrada Dona Castorina 110, 22460 Rio de Janeiro, RJ, Brazil
E-mail address: marchesi@impa.br

Complex Systems Group, Los Alamos National Laboratory, Los Alamos, NM, USA
E-mail address: plohr@lanl.gov